Accurate *ab initio* intermolecular potentials for dense complex fluids: Dispersion and repulsion

M. GOTTSCHALK

GeoForschungsZentrum Potsdam (GFZ),
Telegrafenberg, 14473 Potsdam, Germany
Section 4.1 (gottschalk@gfz-potsdam.de)

For crustal and mantle conditions equations of state (EOS) valid for fluids with complex compositions are still rare and mostly limited to water-rich chemistries. However, fluid immiscibilities might be quite common for complex fluids at elevated pressures and temperatures. But for the evaluation of equilibria and of processes in connection with fluid phase separation such EOS are required.

Using intermolecular potentials of pure species it had been shown (e.g. [1, 2]) that in principle such EOS can be formulated for mixtures applying mixing rules. The exact nature of the potential parameters and validity of the mixing rules remain uncertain especially at high densities. Furthermore [1, 2] do not consider charged species which are important for geological relevant fluids.

Because of the present deficiencies of EOS for complex fluids, the determination of intermolecular potentials and development of EOS for geo-fluids has been started from scratch. Recent development in computational chemistry has demonstrated that precise potentials can be calculated by *ab initio* methods applying correlation-consistent basis sets.

As a first step the dispersion and repulsion, pair and three-body potentials have been calculated for the noble gases using basis sets of the *aug-cc-pVXZ* type [3]. Besides for the pure species He, Ne, Ar, and Kr potentials of their binary and ternary mixtures have been calculated. It has been found that with high accuracy the pair potentials of mixtures can be predicted from the pure pair potentials u_i with the ε_i potential minimum by applying the following mixing rule:

$$u_{ij(r)} = \left(\varepsilon_i \varepsilon_j\right)^{1/2} \left(\left(\frac{\left(\left(u^{rep}_{i(r)}\right)^{1/3} + \left(u^{rep}_{j(r)}\right)^{1/3} \right)}{2} \right)^3 + \left(u^{dis}_{i(r)} u^{dis}_{j(r)}\right)^{1/2} \right)$$

Application using the derived potentials allows the *Monte-Carlo* simulations and such the generation of *PVT* data and *Helmholtz* free energies by thermodynamic integration, which in turn can be used to formulate future EOS for complex fluids.

[1] Churakov & Gottschalk (2003) *GCA* **67**, 2397-2414.
[2] Churakov & Gottschalk (2003) *GCA* **67**, 2415-2425.
[3] Dunning (2000) *J. Phys. Chem.* **A104**, 9062-9080.

Mineralogy of weathering at Questa Mo Mine, NM: 1. Natural analogs

G.J. GRAF[1], V.W. LUETH[2]*, A.R. CAMPBELL[1] AND K.M. DONAHUE[2]

[1]E&ES Dept. New Mexico Tech, Socorro, NM 87801
[2]NMBGMR, New Mexico Tech, Socorro, NM 87801
(*correspondence: vwlueth@nmt.edu)

Natural hydrothermal scars in the area of the Questa mine, NM, have been used as analogs to assess long-term weathering effects within pyritic mine rock piles. These analogs have undergone weathering-related mineralogical changes for periods up to 4 million years. [1].

Two time-scale dependent chemical weathering systems (sulfide and silicate) have been identified. Weathering is readily apparent in the sulfide mineral related system (pyrite-calcite-gypsum). Pyrite tends to decrease as sulfate minerals become more abundant upward in profiles (Fig. 1). Sulfur and oxygen stable isotopes confirm the weathering origin of the sulfates. Particle size decreases upward, consistent with physical weathering, in part induced by chemical weathering processes.

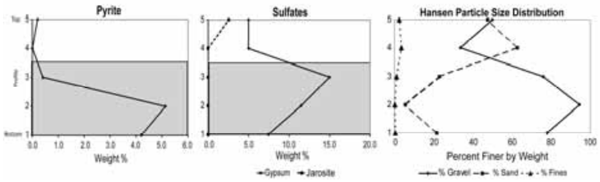

Figure 1: Relative sulfur mineral abundances and grain size variations in weathering profiles. White area = intense qsp alteration. Gray area = qsp overprinting propylitic alteration.

The predominant silicate mineral changes involve total clay and feldspar contents (Fig. 2). However, clay types and mineralogical associations suggest these patterns are due to hydrothermal alteration. Weathering of silicates appears to be limited to dissolution, and the formation of new clays has not been noted.

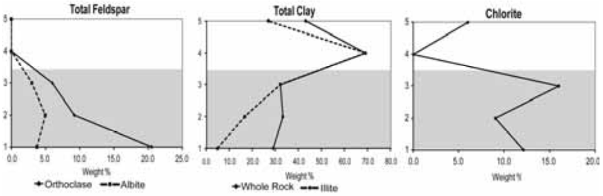

Figure 2: Relative silicate mineral abundance in weathering profiles. Shaded areas, same as Fig. 1.

[1] Lueth *et al.* (2005) *GSA Abs & Prog.* 37, 231.